Grasp Invariance

Alberto Rodriguez and Matthew T. Mason

Abstract This paper introduces a principle to guide the design of finger form: invariance of contact geometry over some continuum of varying shape and/or pose of the grasped object in the plane. Specific applications of this principle include scale-invariant and pose-invariant grasps. Under specific conditions, the principle gives rise to spiral shaped fingers, including logarithmic spirals and straight lines as special cases. The paper presents a general technique to solve for finger form, given a continuum of shape or pose variation and a property to be held invariant. We apply the technique to derive scale-invariant and pose-invariant grasps for disks, and we also explore the principle's application to many common devices from jar wrenches to rock-climbing cams.

1 Introduction

What principles should guide the design of finger form? It depends on context—the specific application, the hand design philosophy, and in particular on the function assigned to the fingers. In this paper we explore the possible role of the fingers in adapting to variations in object shape and pose. One common design approach is to adapt to object shape and pose by control of several actuators per finger. But for simpler hands, with one actuator per finger, or even one actuator driving several fingers, the job of gracefully adapting to shape and pose variations may fall on the finger form. This work explores grasp invariance over shape and/or pose variation as a principle for finger form design.

Alberto Rodriguez
Carnegie Mellon University, Pittsburgh, USA, e-mail: albertor@cmu.edu

Matthew T. Mason
Carnegie Mellon University, Pittsburgh, USA, e-mail: matt.mason@ri.cmu.edu

We begin with a geometry problem:

Scale-invariant contact problem: Given O an object shape in the plane, p a point on the boundary of O, and c the location of the finger's revolute joint, find the finger shape that makes contact at p despite scaling of O.

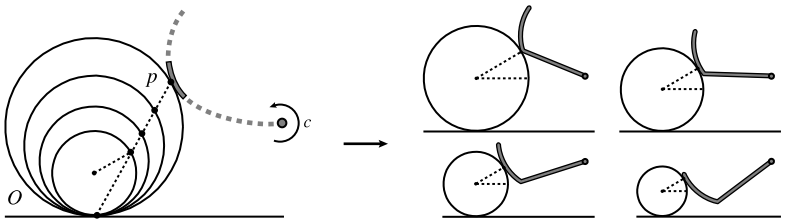

Fig. 1 The scale-invariant contact problem (*left*), solved in Sect. 3.2, yields a finger whose contact with the object O is preserved for different sizes of O (*right*)

If O is a smooth shape, a solution to the previous problem would preserve contact normal as well as contact location. As a consequence, many properties governing the mechanics of grasping and manipulation would also be preserved. For example, as we shall see later in this paper, if O is a disk of varying scale in the palm of a two-fingered hand, the solution of the scale-invariant contact problem yields identical equilibrium grasps despite the variation in scale.

This paper generalizes the scale-invariant contact problem, and explores its implications for finger design for grasping and fixturing problems. Scale-invariant contact is just one example of a broader class of problems where a continuum of constraints guides the design of finger shape. In the specific case of scale invariance, the set of constraints is generated by scaling the object.

In Sect. 3 we show how, under certain conditions, the problem can be mathematically formulated and admits a unique solution as an integral curve of a vector field. In Sect. 4 we find the analytical expression of the integral curve for the most simple and common cases. The integration yields spiral shaped fingers—in special cases, a logarithmic spiral, a shape long noted for its scale invariant properties [11]. Finally, in Sects. 5 and 6, we show that the principle applies to fixture and finger designs seen in many common devices from jar wrenches to rock-climbing cams.

2 Related Work on Finger Design

This paper grew out of our interest in simple hands, focused on enveloping grasps of objects with uncertain pose and shape [9]. The actual forms of the phalanges and the palm become important when the locations of contacts are not carefully planned

and controlled. Simple hands adapt to varying shapes and poses by the emergent interaction of hand with object, rather than by actively driving the hand shape to conform to a known object shape and pose.

Several other approaches are evident in previous hand design literature. The enveloping grasps we employ are often contrasted with fingertip grasps, where the details of phalange form are not usually considered. The dichotomy between enveloping grasps and fingertip grasps corresponds roughly to the distinction between power and precision grasps in Cutkosky and Wright's grasp taxonomy [5].

While much of the analysis of grasp has focused on local stability and in-hand manipulation with fingertip grasps [3], hand design research has explored various grasp types more broadly. The hand design leading to the Barrett Hand [14, 1] explored a single finger probe, a pinch grasp, both cylindrical and spherical enveloping grasps, a two-fingered fingertip grasp, and a hook grasp. The design of the DLR-II likewise was guided by the desire to produce both power and precision grasps [4].

Unlike the work cited so far, our approach does not change the shape of the fingers to adapt to an object pose or shape. Instead, adaptation emerges from the interaction of fixed finger shapes with the object. In that respect the closest work is Trinkle and Paul's [13] work on enveloping grasps, Dollar and Howe's [7] work on hands with compliantly coupled joints, and Theobald et al.'s [10] design of a gripper for acquiring rocks. None of the above focus on the actual finger form. Dollar and Howe [6] survey 20 different designs of compliant and underactuated hands, and all employ cylindrical or straight fingers, occasionally employing some additional shape features, but with no particular principle described to guide their design.

The closest work to this paper is found not in robotics research, but in the design of various tools and hardware. All the devices in Fig. 2 adapt to shape and pose vari-

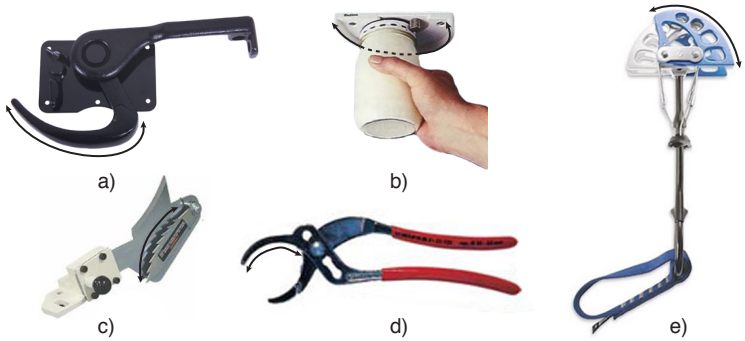

Fig. 2 Curved shapes used in: **a)** Truck door lock; **b)** Jar opener; **c)** Anti-kickback device for table saw; **d)** Pliers; **e)** Climbing cam

ations without changing their shape. Instead, the adaptation arises from the curved shape. In the cases of the rock-climbing cam [8] and the anti-kickback device [2] the shape was derived theoretically. The others, to our knowledge, are product of human intuition. In Sec. 6 we analyze their shape under the grasp invariance principle.

3 Problem Formulation

Let $H(x,s)$ be a parametrized transformation of O, i.e. for all values of the transformation parameter s, $H(O,s)$ is a warped version of the object. We are interested in designing a finger that makes first contact with O at a given point p, and with points $p_s = H(p,s)$ for all warped versions of O. Locally, making first contact is equivalent to the object and finger being tangent. Under this formulation, the scale-invariant contact problem becomes:

> *Transformation-invariant contact problem*: Find the shape of the finger that is always tangent to the set of objects $\{H(O,s)\}_s$ when contacting them at points $\{p_s\}_s$.

Let *contact curve* l describe the travel of the point p, and let *contact vector* v be the tangent to the object at point p, Fig. 3.

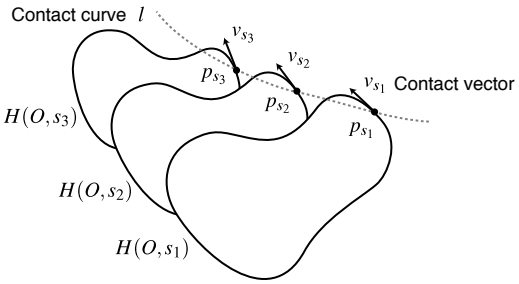

Fig. 3 The motion of the object O defines the travel of the point p and with it, the contact curve l and the motion of the contact vector v

Every point l_s in the contact curve corresponds to an instance of the object, $H(O,s)$. As a consequence it induces a constraint at one point in the finger. This establishes a relationship between points in the contact curve and points in the finger: Whenever the finger crosses the contact curve, i.e. contacts the object at p_s, it must always do it tangent to the corresponding contact vector v_s, i.e. tangent to the object at p_s. In the next section we see that this relation leads to a reformulation of the problem in terms of vector fields.

3.1 Geometric Reformulation of the Problem

The relationship between the finger and the contact curve described in the last section allows us to reformulate the transformation-invariant contact problem as:

> *Transformation-invariant contact problem:* Find the finger form that always crosses the contact curve l tangent to the contact vector v.

Every time the finger crosses the contact curve, its tangent must satisfy one constraint. Let r be the distance between the center of rotation, c, and that contact point. As shown in Fig. 4a, while the finger rotates around c, the same tangential constraint

is propagated along an arc of radius r and center c. By repeating the same procedure for all constraints, or equivalently for all points in the contact curve, we obtain a vector field V defined on an annulus in the plane.

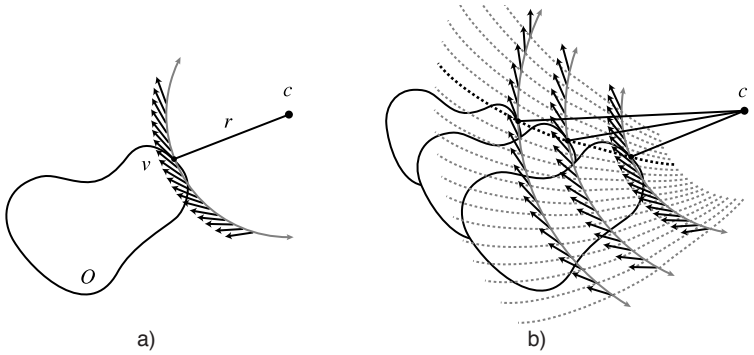

Fig. 4 a) Parallel transport of v radially from c. **b)** Extending the same construction to all values of s, gives us the vector field

The vector field V is well defined if and only if the construction does not impose inconsistent constraints, that is, if and only if it does not impose two different constraints at the same point. To avoid inconsistent constraints, the distance between c and the contact curve must be strictly monotonic, because different points along the contact curve will impose constraints on different concentric arcs. In practice, given a parametrized transformation $H(O,s)$, we avoid inconsistency of constraints by restricting to an interval of s where such distance is strictly monotonic. We will refer to a problem that avoids inconsistent constraints as a *proper problem*.

By construction, any integral curve of the vector field V of a proper problem must satisfy all contact curve constraints. Hence, if we shape the finger following the integral curve, it shall contact the object with the expected geometry, and therefore must be a solution to the transformation-invariant contact problem.

By virtue of the the theorem of existence and uniqueness of maximal integral curves, Theorem 1, the existence of the integral curve depends on the smoothness of the vector field V. If the contact curve l is smooth and v changes smoothly along it, the vector field V will also be smooth because V is the parallel transport of v along concentric arcs centered at c, which is a continuous and differentiable operation. If that is the case, the solution is guaranteed to exist for the restricted interval of s where the problem is a proper problem.

Theorem 1 (Existence and Uniqueness of Maximal Integral Curves). *Let X be a smooth vector field on an open set $U \in \mathbb{R}^{n+1}$ and let $p \in U$. Then there exists a unique and maximal integral curve $\alpha(t)$ of X such that $\alpha(0) = p$.*

The theorem is a direct consequence of the fundamental existence and uniqueness theorem for solutions of systems of differential equations [12].

3.2 General Solution Recipe

The derivation of the previous section suggests a general procedure for obtaining the shape of the finger:

1. Given the parametrized transformation of the object, $H(O,s)$, construct the contact curve l and the set of contact vector constraints v.
2. Obtain the vector field V, by rotating l and v around the rotation center.
3. Find the shape of the finger by integrating V.

Figure 5 shows an example of the procedure applied to the scale-invariant contact problem for a disk-shaped object resting in a planar palm. When scaling the disk, the contact curve l becomes a line and the contact vector v is constant along l.

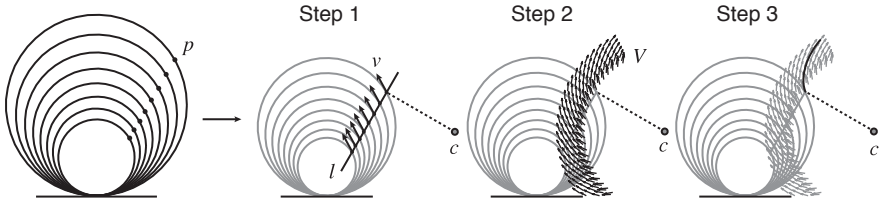

Fig. 5 Step by step execution of the general recipe to obtain the form of the finger for the scale-invariant contact problem . **Step 1** Construction of the contact curve l and contact vectors v. **Step 2** Vector field V. **Step 3** Integral curve of V

4 Analytic Solution

In the general case we can find the shape of the finger using the recipe in Sect. 3.2 and numerically integrating the vector field. In some specific cases, namely when the contact curve l is a line and the contact vector v is constant along it, we can also integrate analytically the vector field. This is the case of linear scaling of the object, translation of the object, or any linear combination of scaling and translation.

Let (x,y) and (r,θ) be the cartesian and polar coordinates in the plane. The shape of the finger is the solution to the system of first order differential equations:

$$\begin{aligned} \dot{x} &= V_x \\ \dot{y} &= V_y \end{aligned} \tag{1}$$

where $V = (V_x, V_y)$ is the vector field obtained in Sect. 3.2. The identity (2) relates the derivatives of the cartesian coordinates to the derivatives of the polar coordinates:

$$\frac{\mathrm{d}y}{\mathrm{d}x} = \frac{r'(\theta)\sin\theta + r(\theta)\cos\theta}{r'(\theta)\cos\theta - r(\theta)\sin\theta} \tag{2}$$

With it, we can rewrite the cartesian system (1) as the single polar differential equation (3) that we will solve in the next subsections.

$$\frac{V_y}{V_x} = \frac{r'(\theta)\sin\theta + r(\theta)\cos\theta}{r'(\theta)\cos\theta - r(\theta)\sin\theta} \tag{3}$$

Without loss of generality we suppose the contact curve l to be parallel to the Y axis and the center of rotation c to lie on the X axis. Let α_0 be the constant angle between l and the contact vector v. Depending on the relative location of c and l we distinguish three cases: (I) c lies on l; (II) c is at finite distance from l; and (III) c is at infinity, i.e. the finger translates rather than rotates.

4.1 Case I: Rotation Center On the Contact Curve

We assume l to be the Y axis and c to be located at the origin as in Fig. 6.

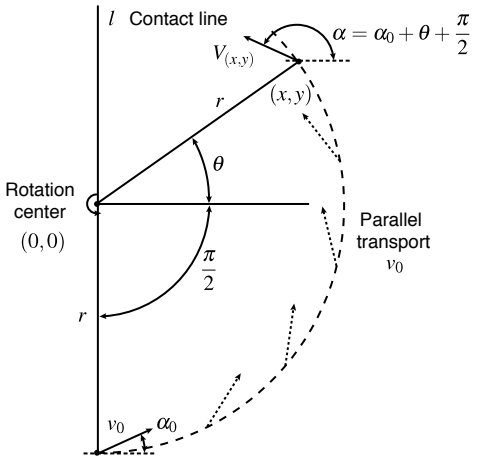

Fig. 6 Parallel transport of v_0 along the arc with center at c gives us $V_{(x,y)}$, the tangent vector to the finger at (x,y)

In this case, the differential equation (3) becomes:

$$\frac{V_y}{V_x} = \tan\left(\alpha_0 + \theta + \frac{\pi}{2}\right) = \frac{r'(\theta)\sin\theta + r(\theta)\cos\theta}{r'(\theta)\cos\theta - r(\theta)\sin\theta} \tag{4}$$

Solving for $r'(\theta)$:

$$r'(\theta) = -r(\theta)\tan\alpha_0 \tag{5}$$

and integrating, we obtain:

$$r(\theta) = \mathrm{C}\, e^{-\theta\tan\alpha_0} \tag{6}$$

where C is the integration constant. Solution (6) is the equation of a logarithmic spiral with pitch $\frac{\pi}{2}+\tan^{-1}(\cot\alpha_0)$. The solution could have been anticipated from the diagram on Fig. 6 because the angle between the radial line and the vector tangent to the curve is constant. This is characteristic of logarithmic spirals and gives them their scale invariant properties [11], as we will further see in Sect. 6.

4.2 Case II: Rotation Center at Finite Distance from Contact Curve

Without loss of generality, let c be the origin and let l be parallel to the Y axis, crossing the X axis at $(1,0)$, as in Fig. 7.

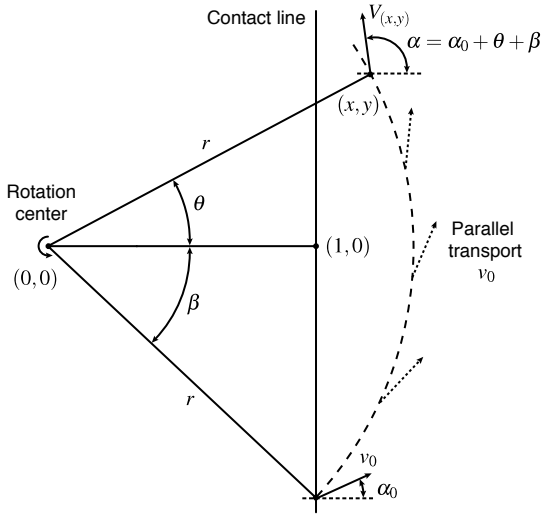

Fig. 7 Same construction as in Fig. 6. Parallel transport of v_0 along the arc with center at c gives $V_{(x,y)}$, the tangent vector to the finger at (x,y)

If we apply (3) to the construction of Fig. 7 we obtain:

$$\frac{V_y}{V_x}=\tan(\alpha_0+\theta+\beta)=\tan\left[\alpha_0+\theta+\cos^{-1}\left(\frac{1}{r}\right)\right]=\frac{r'(\theta)\sin\theta+r(\theta)\cos\theta}{r'(\theta)\cos\theta-r(\theta)\sin\theta} \tag{7}$$

With some trigonometric algebra, (7) can be solved for $r'(\theta)$ as:

$$r'(\theta)=r(\theta)\cdot\frac{\cos\alpha_0-\sqrt{r(\theta)^2-1}\sin\alpha_0}{\sin\alpha_0+\sqrt{r(\theta)^2-1}\cos\alpha_0} \tag{8}$$

Equation (8) is a separable differential equation with form $\frac{\mathrm{d}r}{\mathrm{d}\theta}=g(r)$ and can be solved as $\int \mathrm{d}\theta=\int\frac{1}{g(r)}\mathrm{d}r$:

$$\begin{aligned}
\theta &= \int \mathrm{d}\theta = \int \frac{1}{r(\theta)} \cdot \frac{\sin\alpha_0 + \sqrt{r(\theta)^2-1}\cos\alpha_0}{\cos\alpha_0 - \sqrt{r(\theta)^2-1}\sin\alpha_0}\mathrm{d}r = \left[\begin{array}{c}\text{change}\\ t \to \sqrt{r(\theta)^2-1}\end{array}\right] \\
&= \int \frac{t}{t^2+1} \cdot \frac{(\sin\alpha_0 + t\cos\alpha_0)}{(\cos\alpha_0 - t\sin\alpha_0)}\mathrm{d}t = \\
&= -\int \frac{1}{t^2+1} + \frac{\cos\alpha_0}{\sin\alpha_0 t - \cos\alpha_0}\mathrm{d}t = \\
&= -\tan^{-1}(t) - \frac{\ln(|\sin\alpha_0 t - \cos\alpha_0|)}{\tan\alpha_0} + \mathrm{C} = \\
&= -\tan^{-1}\left(\sqrt{r^2-1}\right) - \frac{\ln\left(|\sin\alpha_0\sqrt{r^2-1} - \cos\alpha_0|\right)}{\tan\alpha_0} + \mathrm{C}
\end{aligned} \tag{9}$$

where C is the integration constant determined by the initial conditions. As shown in Fig. 8, the solution is a family of spirals valid for all α_0, except when $\tan\alpha_0 = 0$. In that specific case, a similar derivation yields a different spiral:

$$\theta(r) = -\tan^{-1}\left(\sqrt{r^2-1}\right) + \sqrt{r^2-1} + \mathrm{C} \tag{10}$$

4.3 Case III: Rotation Center at Infinity

A center of rotation at infinity corresponds to the case where the finger does not rotate but translates in a particular direction v_c, i.e. the finger joint is prismatic rather than revolute. The vector field V is defined, then, by the translation of the contact line in the same direction. As we are limiting the analysis to the case where the contact vector is constant along the contact line, the vector field V is constant on the plane. The integral curve of V, and shape of the finger, is consequently a line segment aligned with the constant contact vector v_0.

The vector field is well defined except in the case when the translation of the finger v_c is aligned with the contact line. In this degenerate situation, the vector field is only defined on top of the contact line, and the solution is still a line.

4.4 Family of Solutions

In cases I and II, the integral curve of the vector field is a spiral. In case III, we always obtain a line segment. Figure 8 shows a summary of the solutions we obtain when changing α_0. Note that the vector fields obtained with α_0 and $\alpha_0 + \pi$ always have the same magnitude and opposite direction, hence it suffices to analyze the range $\left[\frac{\pi}{2}, -\frac{\pi}{2}\right]$. In Fig. 8 we show a long section of the spiral. However, for practical reasons, the actual shape of the finger is just the initial portion.

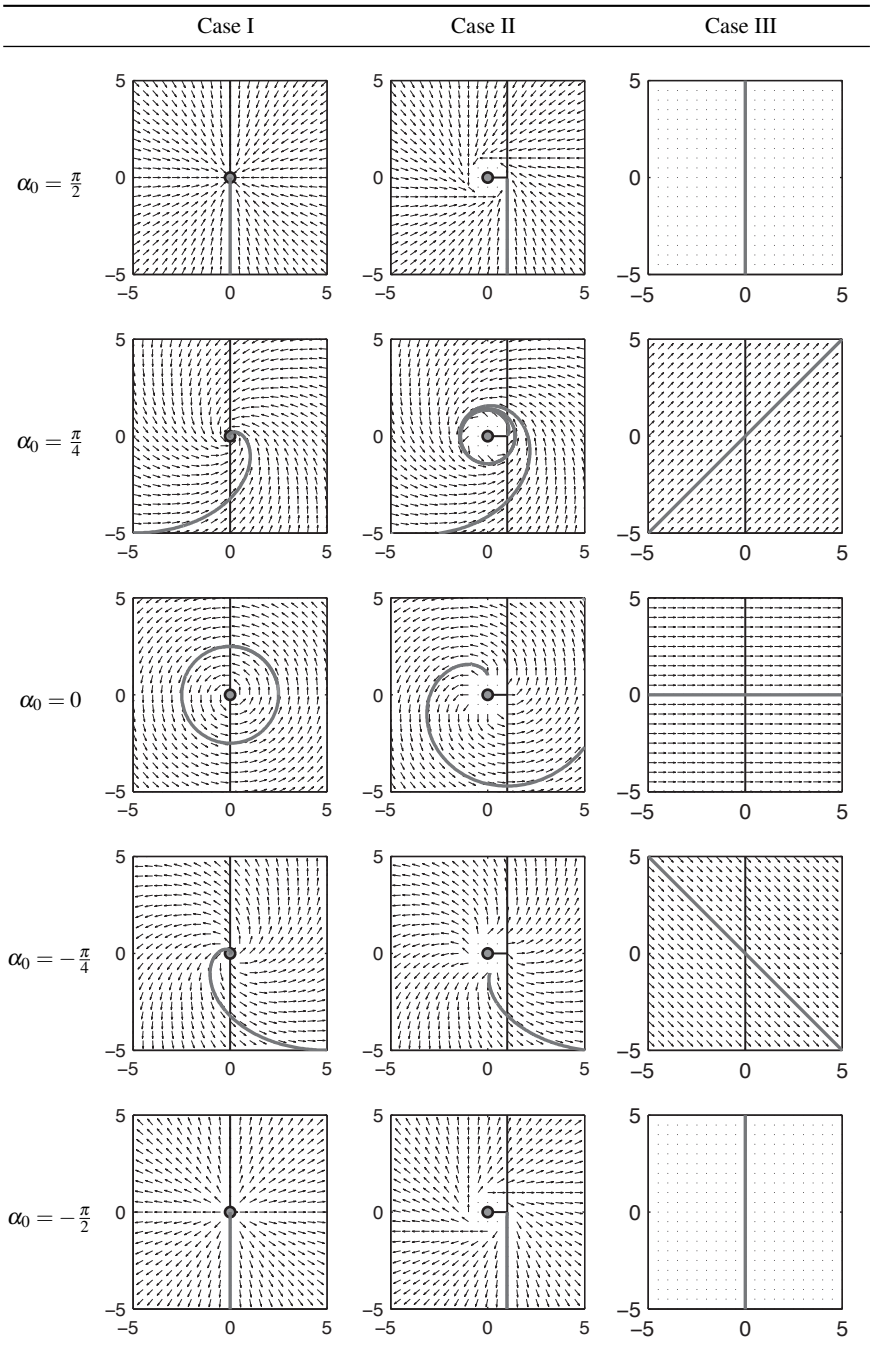

Fig. 8 Plots show the contact curve (*vertical bold line*), the rotation center (*grey dot*), and the finger solution (*grey curves*) for different values of α_0. In all cases, the finger and the contact curve cross at the lower half of the contact curve with constant angle, equal to the corresponding α_0. **Case I** Rotation center lying on the contact curve. **Case II** Rotation center at finite distance from the contact curve. **Case III** Rotation center at infinity

5 Applications to Grasping

5.1 Scale Invariant Grasping

The solution to the scale-invariant contact problem in Fig. 1 shows a finger that contacts a disk of varying size with constant geometry. This same idea can be used to design a gripper whose equilibrium grasps are geometrically invariant with scale. Suppose we aim for a triangular grasp between two fingers and a palm. Fig. 9 shows the corresponding contact line l, contact vectors v, and the induced normalized diagram. The solution belongs to the family of spirals obtained in Case II in Sect. 4.2, where the center of rotation c is at finite distance from the contact line l.

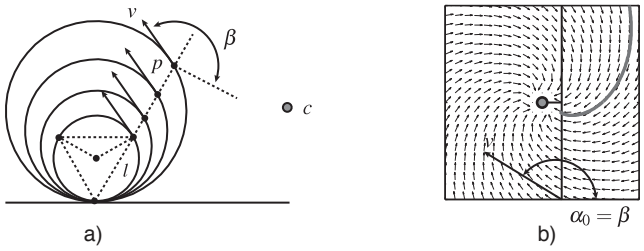

Fig. 9 a) Contact curve, l, and contact vector, v, of the scale invariant grasping application. **b)** Corresponding normalized diagram with $\alpha_0 = \beta$

The contact line, the contact vector, and the form of the finger, depend on the object O and the type of contact we aim for. Therefore, the form of the finger depends on the task to solve. For the specific example of task on Fig. 9, we can construct a scale-invariant gripper by combining two identical but symmetric fingers as in Fig. 10.

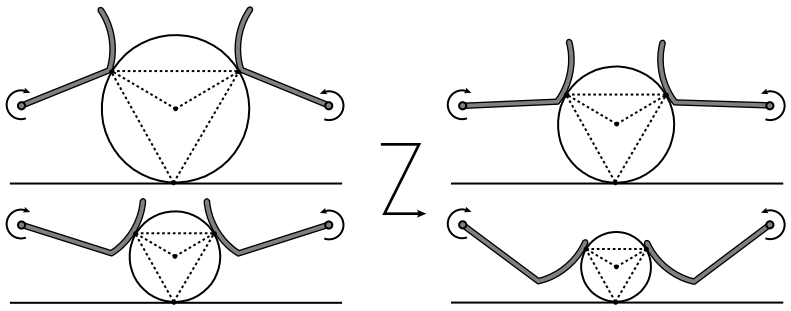

Fig. 10 Gripper with scale invariant fingers for grasping spheres with a regular triangular grasp

5.2 Pose Invariant Grasping

Here we aim to design a hand whose grasps are invariant with respect to the location of a given object rather than scale. Suppose again that we want to grasp a disk of a given size with a triangular grasp, against a planar palm. Now, the disk can be located anywhere along the palm, and we want the grasp geometry to be invariant with respect to that displacement. Figure 11 shows the corresponding contact line l, contact vectors v, and normalized diagram. The solution belongs to the family of spirals in Case II in Sect. 4.2.

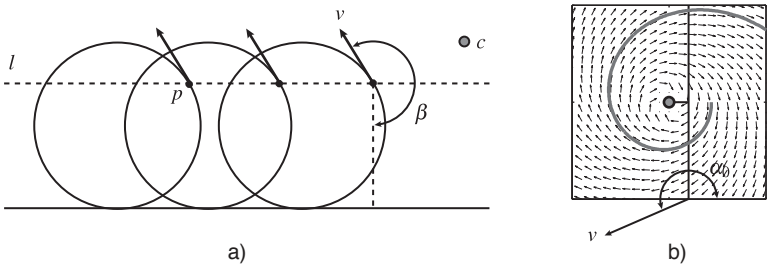

Fig. 11 **a)** Contact curve, l, and contact vector, v, of the pose invariant grasping application. **b)** Corresponding normalized diagram with $\alpha_0 = \beta$

Again, the contact line, the contact vector and consequently the form of the finger depend on the object O and the type of contact desired. The diagram corresponds to case II in Sect. 4.2 with the rotation center at a finite distance from the contact line. In Fig. 12 two identical but symmetric fingers compose a pose-invariant gripper.

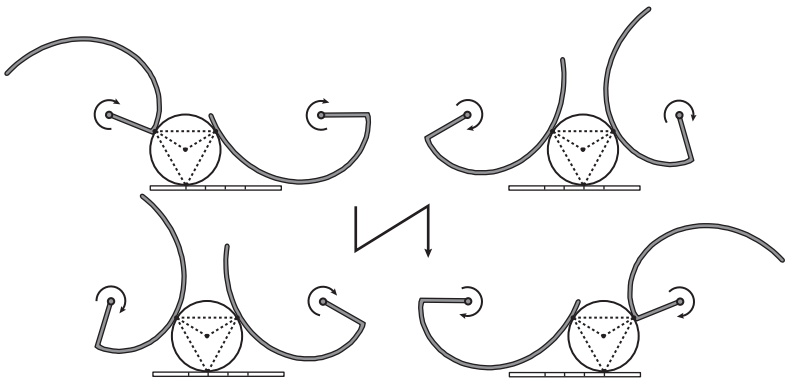

Fig. 12 Invariant grasping geometry for different locations of a sphere

5.3 Pick-up Tool

Suppose we are to design a gripper with two rigid fingers to pick up an object from the ground. The object needs to slide along the length of the fingers while it is being lifted, similar to Trinkle and Paul's work on dexterous manipulation with sliding contacts [13]. Because of the critical role that contact geometry plays in the sliding motion, complex lift plans can be simplified if the contact geometry between finger and object were to be invariant with respect to the lifting motion. With that in mind, we can use the grasp invariance principle to find the finger shape that preserves a contact suitable for sliding. Figure 13 shows a gripper designed to pick up disks.

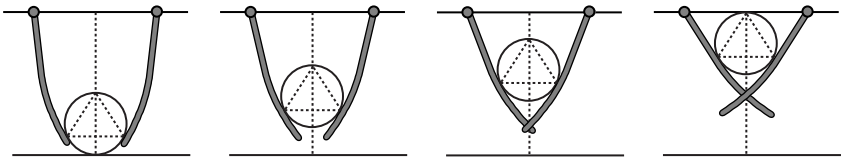

Fig. 13 Invariant contact geometry of the pick-up tool when lifting an object from the ground

6 Applications to Common Devices

6.1 Rock-Climbing Cam

A spring loaded cam is a safety device used in rock climbing to secure anchor points in cracks in the rock face. The device uses the mechanical advantage of the wedge effect to convert pulling force into huge friction forces, Fig. 14.

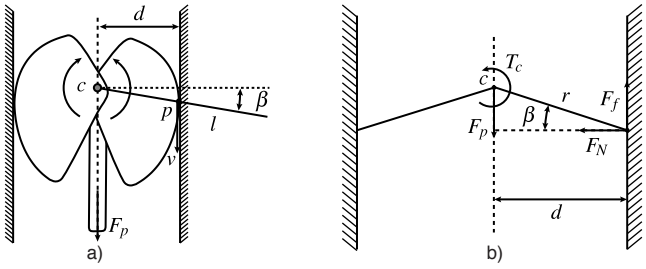

Fig. 14 **a)** Spring loaded cam as used in rock-climbing. **b)** Static force diagram

The diagram on Fig. 14b reveals an important relationship between the coefficient of friction μ and the cam angle β. In static equilibrium (zero torque at c):

$$
\begin{aligned}
& r \cdot F_f \cos\beta = r \cdot F_N \sin\beta \\
\left[F_f \leq \mu F_N\right] \quad & F_N \tan\beta \leq \mu F_N \\
& \beta \leq \tan^{-1}\mu
\end{aligned} \tag{11}
$$

where r is the distance from the cam rotation center c to the contact point, F_N is the normal force caused as a reaction to the pulling force F_p, and F_f is the frictional force. To design a cam whose loading pattern is invariant with the size of the crack, d, we can integrate the constraint (11) so that β remains constant despite variations in d. The rotation center c lies on top of the contact line l and hence the solution is a logarithmic spiral with $\alpha_0 = \beta$ as shown in Fig. 15, example of Case I in Sect. 4.1.

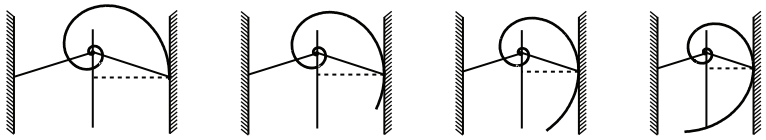

Fig. 15 Invariant loading pattern for different wall openings when using a logarithmic spiral shape

The logarithmic spiral has been used for decades in the design of climbing cams. The invention of modern rock-climbing cams is attributed to Raymond Jardine [8]. His invention used a logarithmic spiral, with camming angle $\beta = 13.5°$.

6.2 Anti Kickback Device for Table Saws

Table saw kickback happens when the blade catches the workpiece and violently throws it back to the front of the saw, towards the operator. An anti kickback device is a passive device that only allows forward motion of the workpiece. Among several options to introduce the asymmetry, one option is to use a spiral like rotating part that wedges a workpiece trying to move backwards, Fig. 16.

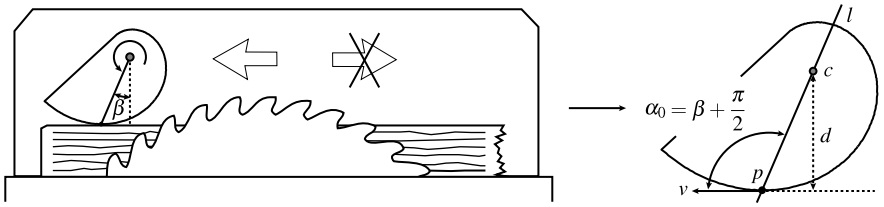

Fig. 16 Anti kickback device as used in a wood table saw. The contact between the retaining part and the workpiece is at an optimum angle β

Experiments have determined that the optimal contact between the workpiece and the anti kickback device is reached when $\beta = 8^\circ$ [2]. To make the contact invariant with the thickness of the workpiece, we can use the grasp invariance principle to design the shape of the device. The center of rotation lies on top of the contact line l and consequently the optimal solution is a logarithmic spiral, with $\alpha_0 = \beta + \frac{\pi}{2}$. The patent of the device [2] proposed a logarithmic spiral as the optimal contour.

6.3 Jar Wrench

The jar wrench in Fig. 2b can open jars of varying sizes. Figure 17 shows the basic operating principle. The lid contacts the inner disk and the outer contour at different places for different sized lids. The mechanics of the opening procedure, and specifically the amount of friction available, depend of the value of the angle β.

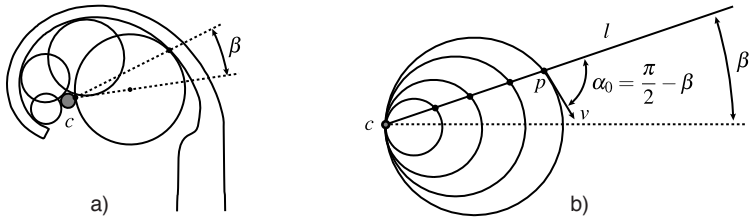

Fig. 17 **a)** Jar wrench. **b)** Simplified diagram where the discs are fixed and the wrench rotates

If we know the optimal value of β, and want the mechanics to be invariant across the range of jar lid sizes, we can use the grasp invariance principle to design the contour. To simplify the analysis we suppose, as shown in Fig. 17b, that the lids are fixed and resting always against the same contact point, while the wrench rotates to contact the lid. The center of rotation is on top of the contact line l. Consequently the optimal shape of the jar wrench is a logarithmic spiral, with $\alpha_0 = \frac{\pi}{2} - \beta$.

7 Discussion

In this paper we have introduced the grasp invariance principle and have given a recipe to apply it to design the form of rotating fingers and fixtures, given a continuum of shape or pose variation and a property to be held invariant. We have shown that, in simple cases, the finger has a spiral form, and have applied the technique to design scale-invariant and pose-invariant grippers for disks and a pick-up tool. Finally we have analyzed the shape of few common devices under the principle.

There are lots of extensions, generalizations and applications that we lacked either the space to discuss or the time to explore. Here we mention a few of them:

- Open design questions: Where should we put the center of rotation c? How do we choose the transformation $H(x,s)$ function? The finger shape depends both on c and $H(x,s)$. Those parameters can be chosen to satisfy additional properties.
- This paper covers design issues of rotating and prismatic fingers. There are other types of finger motion worth considering, for example those involving linkages.
- 2D designs are readily adapted to design grasp invariant 3D grippers, for example by arranging three fingers symmetrically around a circular palm. However we can also think about a deeper 3D generalization where fingers become 2D surfaces.
- What happens when we deal with non-smooth boundaries? Can we extend the approach to include contact at vertices?
- The grasp invariance principle applies to one-dimensional variations of shape or pose of the object, e.g. scale-invariant or pose-invariant grippers. How can we trade off various objectives to address generalization across objects and tasks?

Acknowledgements This work was supported by NSF, ARL and Caja Madrid. This work is sponsored in part by the U.S. Army Research Laboratory, under the Robotics Collaborative Technology Alliance. The views and conclusions contained in this document are those of the authors and should not be interpreted as representing the official policies of the Army Research Laboratory or the U.S. Government. Alberto Rodriguez is the recipient of a fellowship sponsored by Caja Madrid.

References

1. Barrett Technologies: The Barrett hand. `http://www.barrett.com/robot/products-hand.htm` (2001)
2. Berkeley, J.: Anti-Kickback System. US Patent 4,615,247 (1986)
3. Bicchi, A., Kumar, V.: Robotic grasping and contact: A review. In: International Conference on Robotics and Automation, pp. 348–353. IEEE (2000)
4. Butterfass, J., Grebenstein, M., Liu, H., Hirzinger, G.: DLR-Hand II: next generation of a dextrous robot hand. In: International Conference on Robotics and Automation, pp. 109–114. IEEE (2001)
5. Cutkosky, M.: On grasp choice, grasp models, and the design of hands for manufacturing tasks. Transactions on Robotics and Automation **5**(3), 269–279 (1989)
6. Dollar, A., Howe, R.: Joint coupling design of underactuated grippers. In: 30th Annual Mechanisms and Robotics Conference, pp. 903–911. Harvard University (2006)
7. Dollar, A., Howe, R.: The SDM Hand : A Highly Adaptive Compliant Grasper for Unstructured Environments. International Journal of Robotics Research pp. 1–11 (2010)
8. Jardine, R.: Climbing Aids. US Patent 4,184,657 (1980)
9. Mason, M., Srinivasa, S., Vazquez, A., Rodriguez, A.: Generality and simple hands. International Journal of Robotics Research **In review** (2010)
10. Theobald, D., Hong, W., Madhani, A., Hoffman, B., Niemeyer, G., Cadapan, L., Slotine, J., Salisbury, J.: Autonomous rock acquisition. In: Forum on Advanced Developments in Space Robotics. AIAA (1996)
11. Thompson, D.W.: On Growth and Form. Cambridge University Press (1961)
12. Thorpe, J.: Elementary Topics in Differential Geometry, pp. 8–10. Springer (1979)
13. Trinkle, J., Paul, R.: Planning for dexterous manipulation with sliding contacts. The International Journal of Robotics Research **9**(3), 24–48 (1990)
14. Ulrich, N., Paul, R., Bajcsy, R.: A medium-complexity compliant end effector. In: International Conference on Robotics and Automation, pp. 434–436. IEEE (1988)